Internal report to E89-003 collaboration

Updated Normalization Factors and A_{LT} for $^{16}\mathbf{O}(e,e'p)(1p)^{-1}$

James J. Kelly

Department of Physics, University of Maryland, College Park, MD 20742

(Dated: *October 18, 2002)*

In October 1999 I made a survey of the normalization factors needed to fit data for p-shell knockout from ^{16}O obtained in several experiments, expecting that that study would represent one section of a PRC paper to be prepared shortly thereafter. Three year later that paper finally appears to be approaching completion, but the previous calculations are now obsolete. Here I update the previous analysis using similar model input but now using fully relativistic calculations – the effective momentum approximation is no longer needed for spinor distortion. The second significant change is that the normalization factors are obtained by least-squares fitting to data for $|p_m| \leq 200$ MeV/c rather than by eye.

All of the data were analyzed using the same models.

bound-state wave function	NLSH or HS
optical model	EDAIO or EDAD1
electron distortion	EMA
vertex function	$\bar{\Gamma}_2$
form factors	MMD
gauge	Coulomb

The kinematics of the available data are summarized in Table I and the explanatory remarks below.

- Leuschner: the data were provided and analyzed in the form of reduced cross sections. The $1p_{3/2}$ state was resolved.

- Spaltro: the data were provided and analyzed in the form of reduced cross sections. The $1p_{3/2}$ state was resolved. The normalization factors are based upon data for the highest beam energy.

- Chinitz: the data were provided and analyzed in the form of differential cross sections. For the $1p_{3/2}$ state I used data corrected for the positive-parity contamination by the authors.

- Gao: the data were provided and analyzed in the form of differential cross sections. The normalization factors are based upon data for the highest beam energy. The positive-parity contribution to the 6.32 MeV peak was computed using the parametrizations of Leuschner *et al.* and added incoherently to the $1p_{3/2}$ contribution.

TABLE I: Summary of kinematical conditions for various experiments.

panel	experiment	type	T_p	Q^2	x
a	Leuschner	$\parallel$	96		
b	Spaltro	$\perp$	84	0.20	1.07
c	Chinitz	$\perp$	160	0.30	0.91
d	Gao	$\perp$	427	0.80	0.96
e	Bernheim	$\perp$	100	0.19	0.90
f	Blomqvist 1	$\parallel$	92	0.08	0.3 – 0.5
g	Blomqvist 2		215	0.04 – 0.26	0.07 – 0.7

- Bernheim: the data were provided and analyzed in the form of reduced cross sections. The positive-parity contribution to the 6.32 MeV peak was computed using the parametrizations of Leuschner *et al.* and added incoherently to the $1p_{3/2}$ contribution.

- Blomqvist: two experiments with rather different kinematics are included; the $1p_{3/2}$ state was resolved. The data were provided and analyzed in the form of reduced cross sections. Calculations were made for each point in these data sets. The kinematics for $T_p \approx 215$ MeV were highly varied.

Fits for four combinations of optical potential and bound-state wave function are shown in Figs. 1–4, where the panels are labeled according to Table I. The HS wave function provides a better fit than NLSH to the low Q^2 data, especially for the Leuschner experiment. However, the NLSH wave function appears to fit the Gao data better, but the coverage of the missing momentum distribution is so sparse for our experiment that I am inclined to prefer the HS wave function. Plane wave momentum distributions for these models are compared in Fig. 5. One finds little difference for $1p_{3/2}$ but an appreciable difference for the ground state. Note that even better fits to the Leuschner p_m distributions can be obtained using Woods-Saxon wave functions, but I have not updated those calculations since incorporation of relativistic dynamics into the model. I believe that the consistency between theory and experiment can be improved by fitting bound-state wave fucntions rather than relying upon relativistic mean-field (RMF) theory optimized for heavier nuclei. Although NLSH is supposed to be an improvement over the older HS model, light nuclei were not considered and there is no guarantee that it is better for oxygen.

TABLE II: Normlization factors for p-shell knockout. Each column gives factors for the lowest ($1p_{1/2}$,$1p_{3/2}$) states for a particular choice of bswf and optical potential.

experiment	NLSH,EDAIO	NLSH, EDAD1	HS,EDAIO	HS,EDAD1
Leuschner	(0.60, 0.47)	(0.67, 0.57)	(0.55, 0.46)	(0.60, 0.55)
Spaltro	(0.66, 0.69)	(0.78, 0.78)	(0.61, 0.67)	(0.72, 0.76)
Chinitz	(0.61, 0.59)	(0.69, 0.64)	(0.55, 0.57)	(0.60, 0.62)
Gao	(0.74, 0.69)	(0.74, 0.67)	(0.65, 0.66)	(0.65, 0.67)
Bernheim	(0.49, 0.47)	(0.55, 0.54)	(0.43, 0.46)	(0.48, 0.53)
Blomqvist 1	(0.55, 0.42)	(0.59, 0.51)	(0.53, 0.42)	(0.57, 0.51)
Blomqvist 2	(0.44, 0.38)	(0.45, 0.42)	(0.43, 0.38)	(0.43, 0.41)

Similarly, the data show a slight preference for the EDAD1 optical potential over EDAIO. The fit quality is slightly better for EDAD1. The EDAD1 normalization factors are larger for low Q^2 and more consistent. Perhaps a better choice can be found, but the effort does not seem worthwhile at this time.

For the sake of completeness I also compare A_{LT} for these models with the available three data sets in Fig. 6. There is very little sensitivity to the choice of bswf, whereas the Gao data show a slight preference for the EDAIO optical potential; however, this preference is not convincing because the effect is mostly at large p_m where other effects become important also.

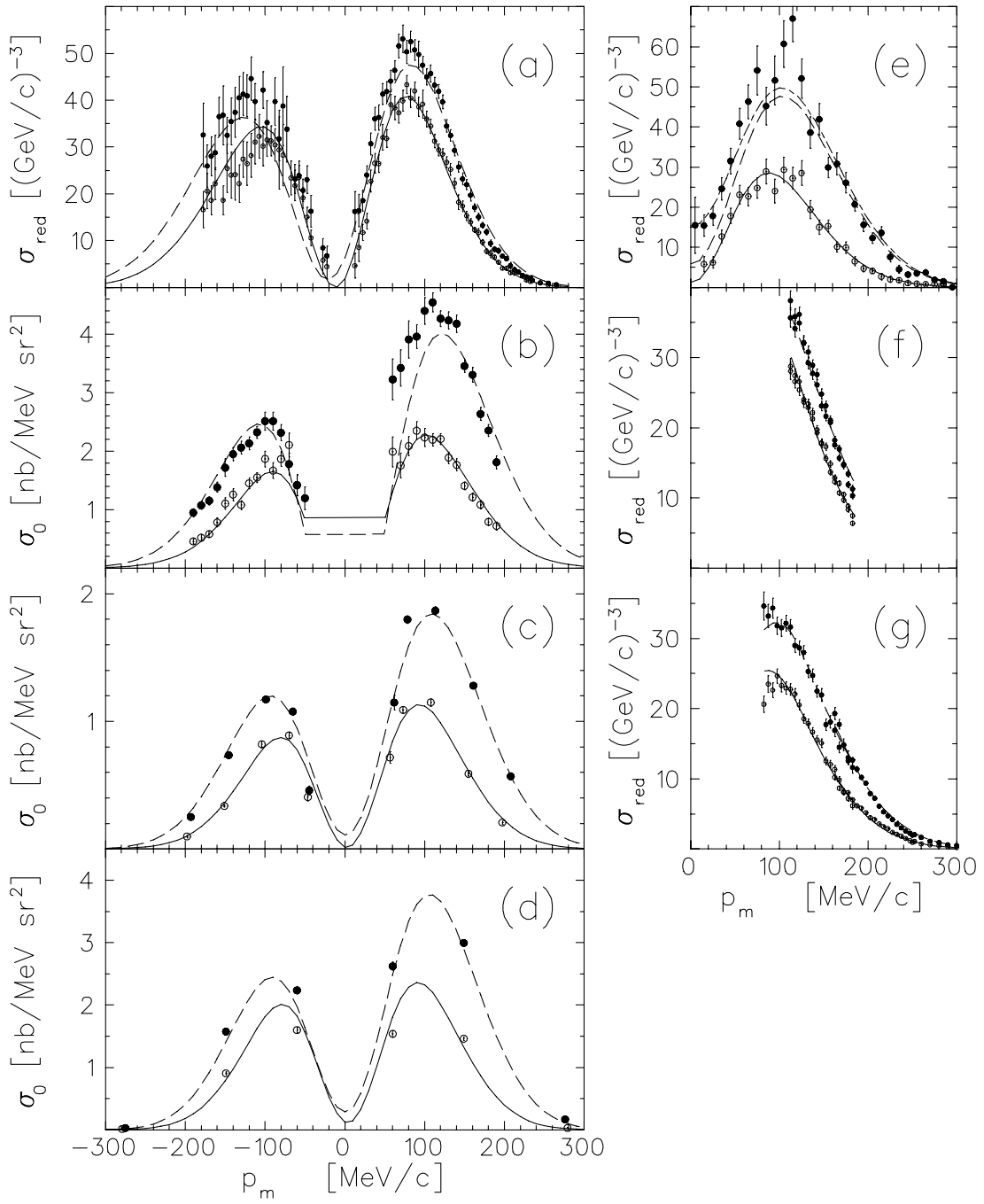

FIG. 1: Scale-factor fits to $^{16}\mathrm{O}(e,e'p)(1p)^{-1}$ data. Open points and solid lines pertain to $1p_{1/2}$, while solid points and dashed lines refer to $1p_{3/2}$. Dash-dotted lines include positive parity contributions to the 6.32 MeV peak. These fits use NLSH wave functions and the EDAIO optical potential.

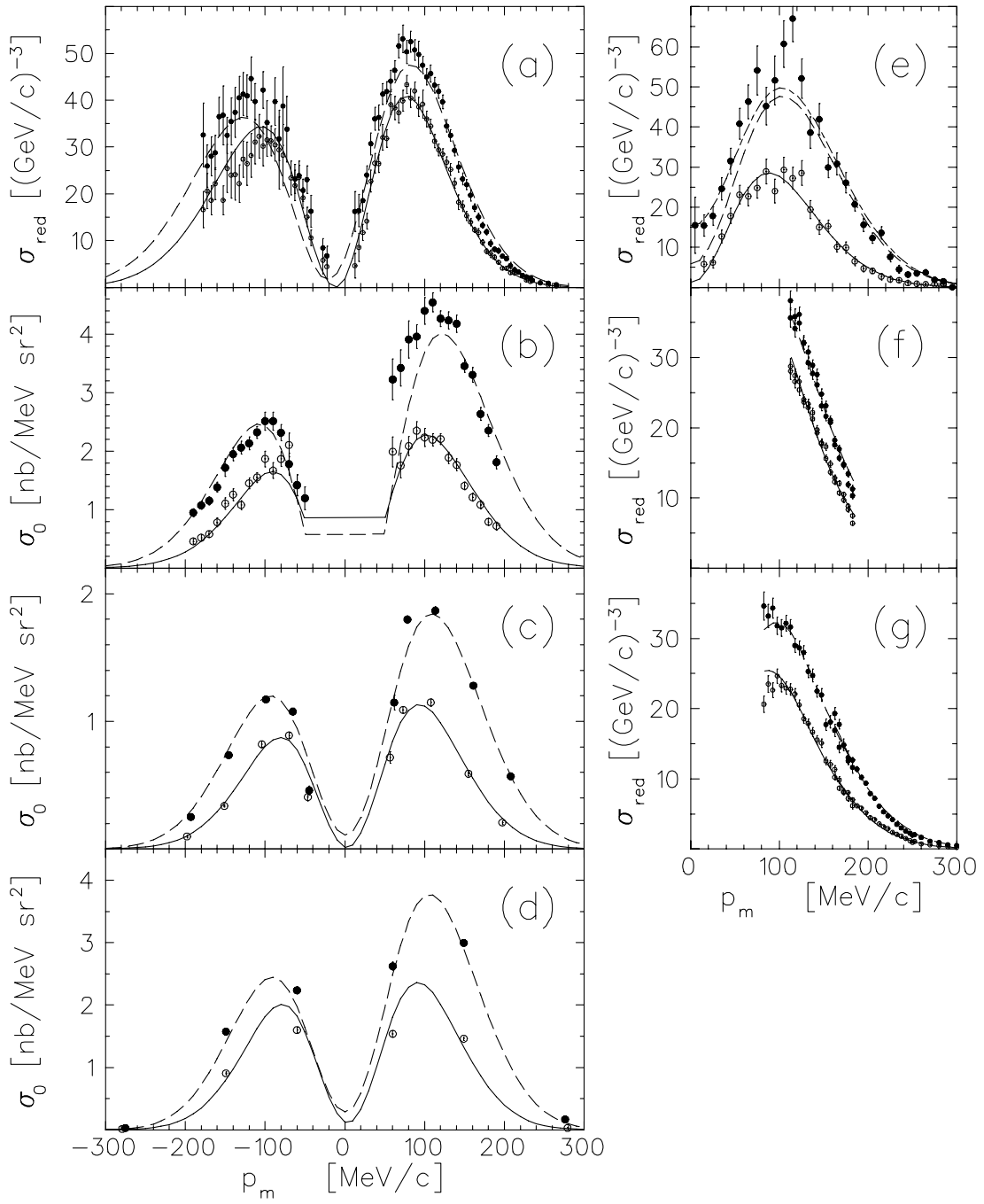

FIG. 2: Scale-factor fits to $^{16}\mathrm{O}(e,e'p)(1p)^{-1}$ data. Open points and solid lines pertain to $1p_{1/2}$, while solid points and dashed lines refer to $1p_{3/2}$. Dash-dotted lines include positive parity contributions to the 6.32 MeV peak. These fits use NLSH wave functions and the EDAD1 optical potential.

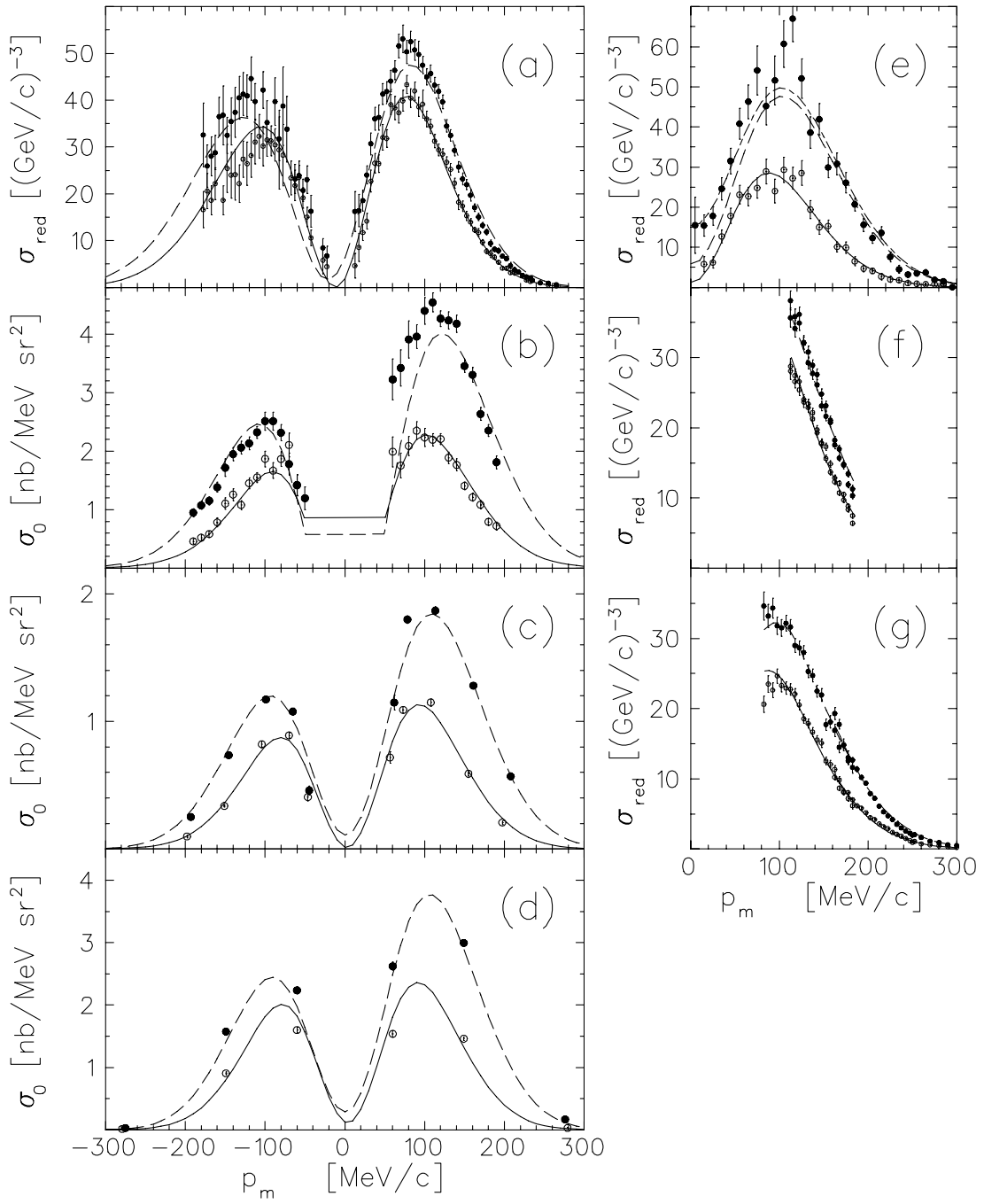

FIG. 3: Scale-factor fits to $^{16}\mathrm{O}(e,e'p)(1p)^{-1}$ data. Open points and solid lines pertain to $1p_{1/2}$, while solid points and dashed lines refer to $1p_{3/2}$. Dash-dotted lines include positive parity contributions to the 6.32 MeV peak. These fits use HS wave functions and the EDAIO optical potential.

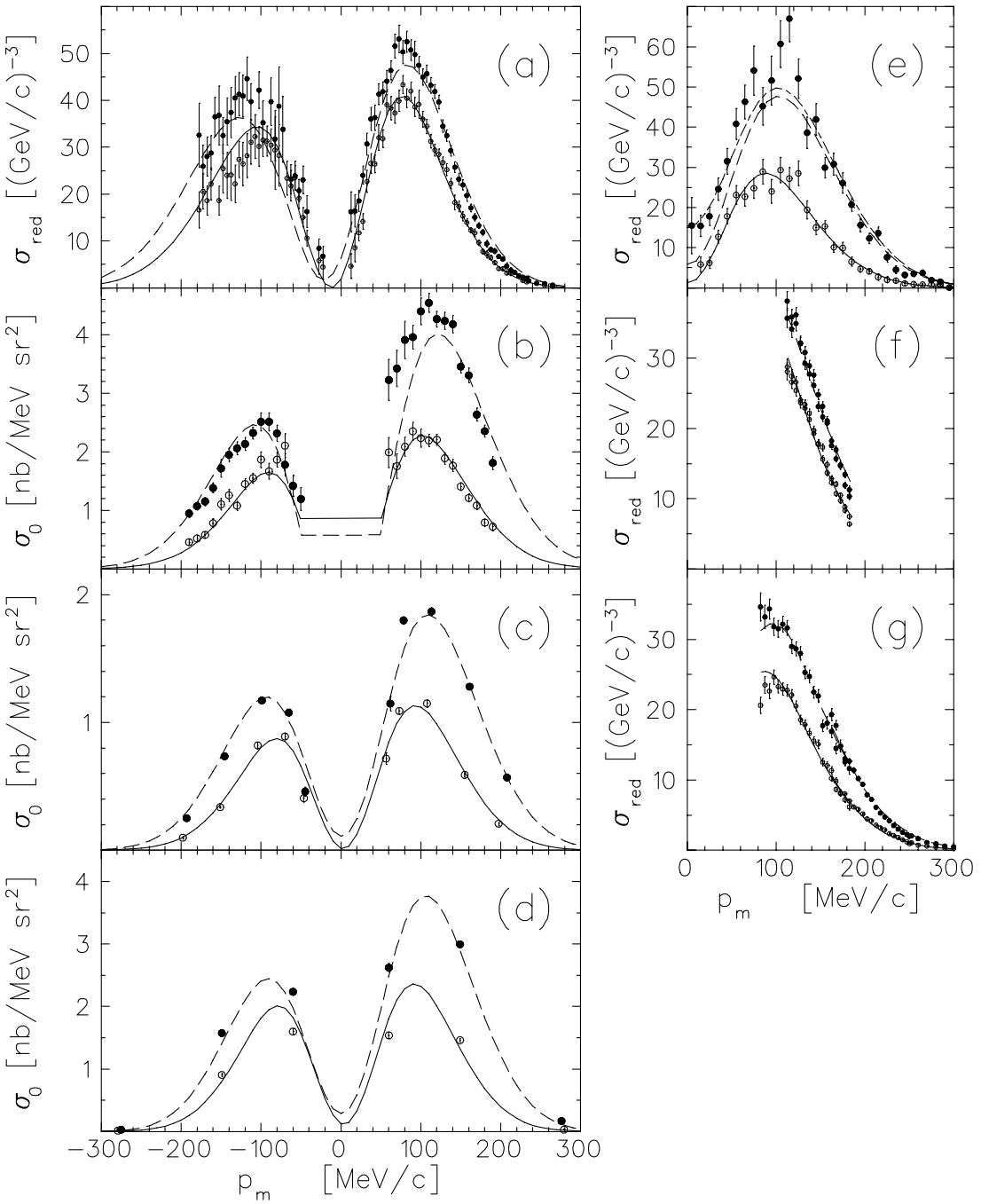

FIG. 4: Scale-factor fits to $^{16}\mathrm{O}(e,e'p)(1p)^{-1}$ data. Open points and solid lines pertain to $1p_{1/2}$, while solid points and dashed lines refer to $1p_{3/2}$. Dash-dotted lines include positive parity contributions to the 6.32 MeV peak. These fits use HS wave functions and the EDAD1 optical potential.

FIG. 5: Comparison between plane-wave momentum distributions for the HS and NLSH models.

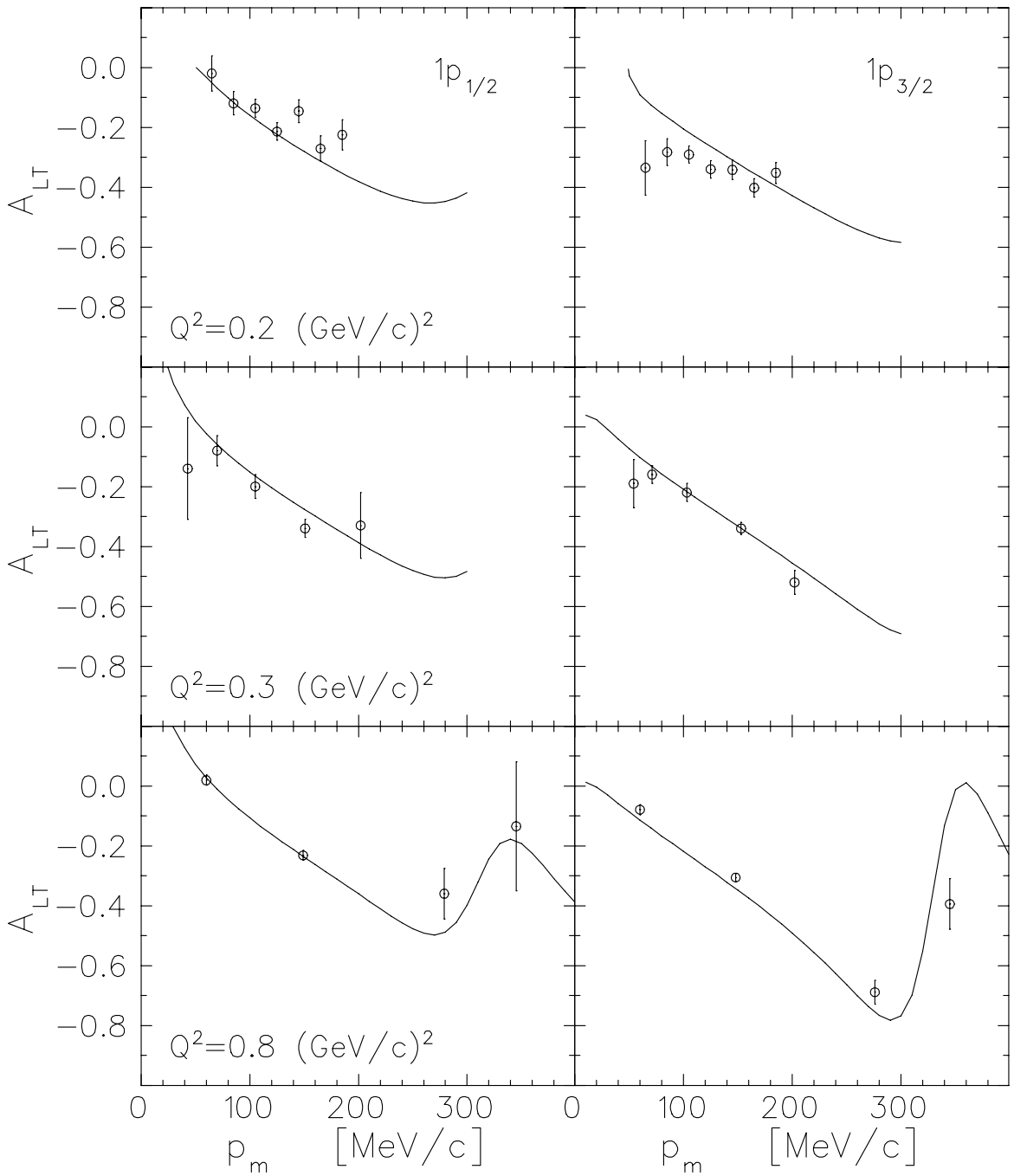

FIG. 6: A_{LT} for $^{16}\mathrm{O}(e,e'p)(1p)^{-1}$.